# MUSCULOSKELETAL SIMULATIONS OF MOTOR RECRUITMENT STRATEGIES

Lai, A.K.M.[1] and Wakeling, J.M. [1]
[1] Neuromuscular Mechanics Laboratory, Department of Biomedical Physiology and Kinesiology, Simon Fraser University, Burnaby, BC, Canada
email: adrian_lai@sfu.ca, web: http://www.sfu.ca/nml.html/

## INTRODUCTION

Mammalian skeletal muscle contains many motor units. The base recruitment plan of these motor units is known as orderly recruitment or "size-principle", which states that motor units are recruited in an orderly fashion where the motor units consisting of the smallest motorneurons are recruited first and the largest are recruited last [1]. In addition, the contractile properties of the muscle fibres that belong to each motor unit can vary, being broadly categorised as slow and fast-twitch fibres. Hence, the population of motor units that are recruited and the contractile properties of the muscle fibre types influence the dynamics of a muscle contraction. Musculoskeletal simulations are commonly used to predict muscle function and coordination strategies during movement. However, many muscle models consider neither the heterogeneity of fibre type properties nor motor recruitment strategies.

In this study, we introduce a predictive simulation framework that accounts for the contractile properties and motor recruitment patterns of different fibre types. We test the effectiveness of the framework to predict physiological motor recruitment patterns by simulating a ramped isometric contraction using a lower limb model and two physiological cost functions.

## METHODS

We used a similar approach to Lai et al. [2] where an existing musculoskeletal model was adapted to include the right thigh, shank and foot segments and three Hill-type actuators: two plantarflexors and a dorsiflexor. Each actuator contained a contractile element with normalised active and passive force-length-velocity properties [3]. The series elastic element of the plantarflexors were assumed to be rigid and hence, the two plantarflexors were analogous to two parallel muscle fibres within a muscle that could have different fibre types. To simulate the contractile properties of different muscle fibre types, we varied the maximum contraction velocity, the curvature of the force-velocity relationship and the activation and deactivation time constants of the excitation-to-activation dynamics. The muscle fibres were assigned properties that represented fast and slow-twitch fibres.

To generate predictive, dynamic optimisation simulations, we developed a simulation framework where we solved an optimal control problem using direct collocation methods. We interfaced OpenSim (v 3.3 [4]), an interior point optimiser [5] and MATLAB to solve for a set of neural excitations and state variables (e.g. joint angles) that minimised a cost function while satisfying a set of constraints that represented the system dynamics. The mixed cost function contained a data-tracking and a physiological term. The data tracking term drove the simulations towards the desired kinematics. To test the effectiveness of the framework to predict motor recruitment patterns during a ramped isometric contraction, two physiological terms were implemented and compared: (1) minimise the sum of activations squared; (2) minimise metabolic cost [6]. A typical ramped isometric contraction was simulated where all the joints were held constant and a hypothetical ramped up and down external force was applied to the foot segment of the model over 1.5 seconds.

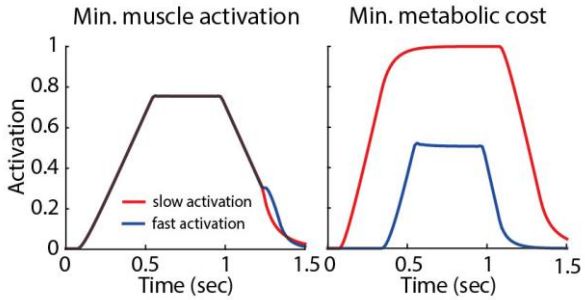


Figure 1: Muscle activations of the slow and fast fibres using the two cost functions during the simulated ramped contraction.

## RESULTS AND DISCUSSION

The framework predicted physiological muscle activations that were consistent with orderly recruitment during the simulated contraction when the cost function containing metabolic cost was implemented. Specifically, the slow muscle fibres were recruited first and fast fibres were recruited only when the slow fibres were unable to generate sufficient force against the external ramped force (Fig. 1). Moreover, the fast fibres were derecruited before the slow fibres, consistent with the orderly decruitment principle. In contrast, when the commonly-used cost function of minimising muscle activations was implemented, the slow and fast muscle fibres were activated and deactivated synchronously, which was inconsistent with orderly recruitment.

We were able to show that our simulation framework, with a metabolic-based cost function, was capable of predicting physiological motor recruitment patterns if the heterogeneity of muscle fibre type properties were considered. Future work will use the framework to predict motor recruitment strategies during dynamic movement tasks especially in tasks where fibre strain rates are varied such as during pedalling across a range of cadences.

## REFERENCES

1. Henneman E, et al., *J. Neurophysiol.* **28**, 560–580, 1965
2. Lai AKM, et al., *J Biomech* **68,** 6-13, 2018.
3. Millard M, et al., *J Biomech Eng.* **135**, 1-11, 2013.
4. Delp S, et al., *IEEE Tran. Biomed. Eng.* **54**, 1940-1950, 2007.
5. Wachter A, et al., *Math Prog.* **106**, 25-57, 2006.
6. Minetti A, et al., *J Theo. Biol.* **186**, 467-476, 1997.

# COMPARISON OF MACHINE LEARNING ALGORITHMS FOR ACTIVITY CLASSIFICATION USING EMG

Anderson, A.J.[1,2], Schuster, E.D.[1,2], Willson, A.M.[1,2] and Aubin, P.M.[1,2]
[1] Department of Mechanical Engineering, University of Washington, Seattle, WA, USA
[2]VA Puget Sound RR&D Center for Limb Loss and MoBility (CLiMB), Seattle, WA, USA
email: ajanders@uw.edu, web: http://faculty.washington.edu/paubin/wordpress

## INTRODUCTION

Abundant wearable sensor data and advances in machine learning algorithms have made activity classification a viable technique for biomechanical studies. Research groups have used different classification algorithms to predict gait activities using lower-limb electromyography (EMG), but few studies have compared the effectiveness of common classification algorithms [1,2]. The purpose of this experiment was to evaluate the predictive performance of four commonly used pattern recognition algorithms on a labeled EMG dataset of six mobility tasks of daily living.

## METHODS

With approval from the VA Puget Sound Health Care System's IRB, EMG data was recorded for two subjects (male, age 24-27, height 5'10"-6'2") at the VA Center for Limb Loss and Mobility. For each subject, 16 EMG sensors (Delsys Inc., Natick MA) were placed on the right leg and lower abdomen. Ten of the sensors were placed on leg muscles commonly measured in EMG studies. The six remaining sensors were placed pseudo-randomly, without isolating specific muscles. All sensors streamed data to a desktop PC at 1200 Hz for the duration of the study. For both subjects, 150 trials lasting three seconds were recorded while the subject performed each of the following activities: standing, sitting, walking at a self-selected pace, walking at 175% of the self-selected pace, stair ascent, and stair descent.

Using MATLAB (MathWorks, Natick MA), each three-second recording was separated into 0.15-second windows. Each window contained signals from all 16 sensors and was labeled as one of the six activities. The following five features were then extracted for each sensor over each of the 0.15-second snapshots: mean average value, number of zero crossings, variance, number of slope sign changes, and waveform length. These five features across 16 sensors resulted in an 80-dimensional feature vector for each window.

The data was then randomly split into a training set (80% of data) and a testing set (20% of data). The training data was reduced via SVD to a collection of 40-dimensional feature vectors. These labeled vectors were then used to train the following classification algorithms: a random forest (RF) with 40 decision trees, a linear support vector machine (SVM), linear discriminant analysis (LDA), and an artificial neural network (ANN) with 100 neurons in a single hidden layer. Each classifier was then tested on its ability to accurately predict the activities in the testing dataset.

This train-test process was repeated ten times with a different random 80-20 cut of the initial dataset each time. The classifiers were trained on an individual basis, i.e. trained with participant 1's data and tested with participant 1's data, as well as on a group basis where the classifiers were both trained and tested with both participants' data.

To determine how classification accuracy was impacted by removing sensors from the initial dataset, a standard backward-removal algorithm was implemented for each classifier.

## RESULTS AND DISCUSSION

All the classifiers predicted the activities with high accuracy (>80%) (Figure 1). The classifier with the highest accuracy when trained and tested with data from both participants was the ANN at 94.95 ± 0.01%.

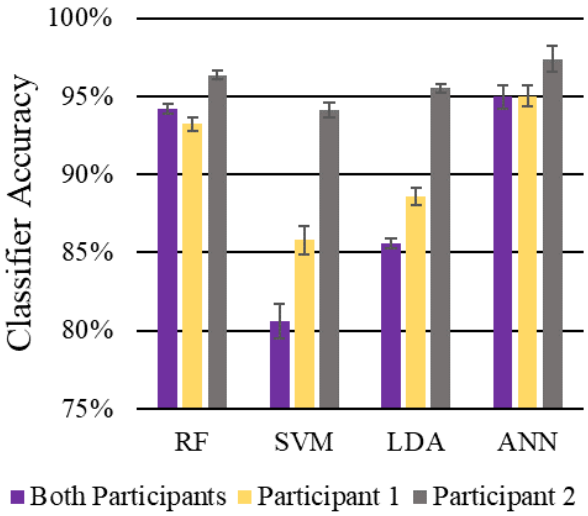


**Figure 1**: Mean classifier testing accuracies when trained on individual and combined subject data with all sensors. Each bar shows the mean of ten cross-validations.

While the accuracy of the ANN was slightly greater than the RF, the backward-selection algorithm showed the RF to be superior, as it could achieve over 90% accuracy with only the Tibialis Anterior and posterior mid-shank sensors. The ANN required seven sensors to reach a comparable classification accuracy. The backward-selection algorithm also revealed that the classifiers did not rely exclusively on the sensors placed on muscle bellies but used information from the nonconventional sensor placements as well.

These techniques could also be applied with sensors other than EMG, including IMUs, heart-rate monitors, or a combination of sensor types to improve classifier accuracy. These results can inform future studies on supervisory prosthetic limb control or monitoring patient activity outside of the laboratory environment.

## REFERENCES

1. Hargrove et al. *IEEE Transactions on Biomedical Engineering.* **56**(5). 2009.
2. Huang et al. *IEEE Transactions on Biomedical Engineering.* **58**(10). 2011.

# COMPARISON OF HEEL LINEAR STIFFNESS IN PROSTHETIC FEET

Halsne, E.G.[1,2], Turner, A.T.[1], Caputo, J. [3], and Morgenroth, D.C. [1,2]
[1]Center for Limb Loss and Mobility, VA Puget Sound Health Care System, Seattle, WA USA
[2]Dept. of Rehabilitation Medicine, University of Washington, Seattle, WA USA
[3]Human Motion Technologies, Inc. USA
email: bhalsne@uw.edu; dmorgen@uw.edu

## INTRODUCTION

Prosthetic feet are an important component of restoring mobility in people with lower limb amputations (LLA). Currently, the process for selecting and prescribing prosthetic feet is primarily guided by clinician experience and based on the patient history and physical examination. There is limited objective prosthetic foot performance data available to inform the selection process. An improved understanding of the mechanical properties of prosthetic feet would help prescribing clinicians in choosing a foot that best matches each individual patient's goals, abilities, and the environmental terrains they regularly traverse.

The mechanical properties (e.g., compressive stiffness) of prosthetic feet can be measured using various techniques. For example, investigators have used motion capture data while an amputee is walking in a laboratory to measure prosthetic foot stiffness [1]. While this technique of data collected is ecologically valid (i.e., measuring foot properties during intended use), the results are confounded by individual gait variation, and do not allow for standardization of testing across different foot types. Other studies have collected foot stiffness data using linear compression ex vivo (i.e., mechanical testing) at discrete angles of loading, but have not collected data on heel stiffness [2]; an additional prior study measured linear stiffness across different categories within a single type of foot [3]. However, there is limited data on performance of the heel component of prosthetic feet across a range of prosthetic foot types.

Therefore, the purpose of this study was to compare the heel linear stiffness across a range of commercially-available prosthetic feet, in an amputee-independent manner.

## METHODS

Data were collected on the following five, size 28cm, prosthetic feet with matched patient weight stiffness categories: Walk-tek (Freedom Innovations, Irvine, CA), Seattle Lightfoot 2 (Trulife USA, Jackson, MI), Vari-flex (Össur, Reykjavik, Iceland), RUSH87 (Ability Dynamics, Tempe, AZ), and All-pro (Fillauer, Inc, Chattanooga, TN).

Apparatus: A Mikrolar R2000 robot and an 8-camera Vicon motion capture system were used to collect linear displacement of prosthetic feet. A 6-axis AMTI load cell was used to collect force data in parallel with the prosthetic pylon.

Procedures: Each foot was attached in line with the load cell, shod with a standardized walking shoe, and fixed to the R2000 robot in neutral alignment in all planes. Procedures included quasi-static testing at a single, discrete pylon progression angle (i.e., -10º) to isolate loading of the heel components. Each foot was compressed for five cycles of loading and unloading to a load threshold representative of average body weight for the tested weight category (i.e., 800N) and the final three cycles were averaged.

## RESULTS AND DISCUSSION

Vertical force vs. displacement profiles depicting loading and unloading of the prosthetic feet were compared (Figure 1).

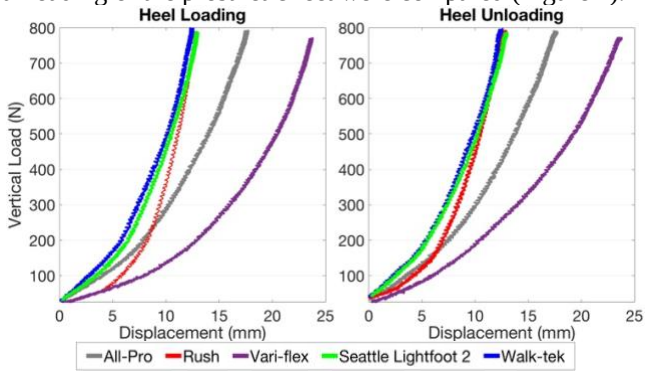


Figure 1: Vertical load vs. displacement across five types of feet. 1a) loading portion; 1b) unloading portion.

The Vari-flex foot demonstrated the lowest stiffness (i.e., greatest displacement) during loading and unloading relative to the other feet tested. In contrast, the Seattle Lightfoot 2 and Walk-tek demonstrated the highest stiffnesses. The RUSH foot exhibited low heel stiffness during early loading, followed by an evident increase in stiffness at approximately 200N, which corresponds to contact between the heel platform and an elastomeric wedge within the heel element. The Walk-tek and Seattle Lightfoot2 demonstrated similar stiffness inflection points, while the Vari-flex and All-pro had relatively uniform curvilinear stiffness profiles throughout the complete loading cycle.

## CONCLUSIONS

Vertical loading vs. displacement curves produced using this method provides prosthetic heel stiffness data in a user-independent manner. Heel stiffness is an important feature affecting loading response during the early stance phase of gait; optimizing this variable can potentially modify residual limb shock absorption, reduce distal anterior residual limb pain and improve overall gait quality. These findings are an important step in developing a library of objective data on prosthetic foot mechanical properties that have great potential to help inform prosthetic foot prescription, thus helping to improve functional mobility in people with LLA.

## REFERENCES

1. Hansen. *J Prosthet Orthot*, **17**, S23-29, 2005.
2. Major, et al. *J Biomech*, **44**(14), 2572-2575, 2011.
3. Morgenroth, et al. *AAOP Conference Proceedings*, 2012.

## ACKNOWLEDGEMENTS

This research was supported through Department of Defense award number W81XWH-16-1-0569.

# CONSTRUCTION PROCESS OF BONE PHANTOMS FOR BIPLANE FLUOROSCOPY VALIDATION

Chastain, K.L.[1,2], Kindig, M.W.[1], Thorhauer, E.D.[1,2], Ricketts, A.A.[1,3], and Ledoux, W.R.[1,2,4]
[1]RR&D Center for Limb Loss and MoBility, VA Puget Sound Health Care System, Seattle, WA,
Departments of [2]Mechanical Engineering, [3]Bioengineering and [4]Orthopaedics and Sports Medicine,
University of Washington, Seattle, WA
email: kchas21@uw.edu, web: http://www.amputation.research.va.gov

## INTRODUCTION

Biplane fluoroscopy is an alternative to motion capture that is becoming increasingly popular in the biomechanics community. This technique allows one to directly visualize and track the motion of bones. In our laboratory, we have developed a biplane system in which two X-ray fluoroscopes image the foot during walking. The 2D fluoroscope images are then converted to 3D motion using a custom model-based tracking method. Similar methods have been found to track motion less than 0.5 mm of translation and 0.5 deg of rotation for leg bones [1]; however, the small and irregularly-shaped bones of the foot are particularly challenging. The goal of this study is to validate these model-based tracking algorithms through the use of bone phantoms, similar to our previous work [2]. The purpose of this study was to develop robust bone phantoms and exercise them under uniaxial rotation, where an external reference provides a gold standard.

## METHODS

Our bone phantom design involved embedding isolated cadaver foot bones in a surrounding foam material. For each phantom, we extracted a bone from a cadaver specimen and the soft tissue removed with an osteotome and scalpel. A custom potting rig was constructed from two halves of 7.5 cm inner diameter PVC, cut 30 cm long. The bone was anchored in the mold with decking screws such that its anterior-posterior axis was collinear with the long axis of the cylindrical mold. The mold was then filled with a two-part polyurethane foam [Mixes 624/625, Fibre Glast, Brookville, OH, USA]. This foam was chosen for its low radiodensity (approximately 1/8 of bone), high compressive strength when fully cured, and resistance to moisture.

Next, custom radiopaque fiducial markers were constructed. A stainless-steel ball bearing was drilled into an acrylic plug (13 mm diameter x 10 mm long) and glued in place. Each phantom had eight such plugs inserted ~10cm from either end of the phantom: the anterior end had a plug with a 4mm-diameter bearing and three with 2mm-bearings, while the posterior end had 2 each of the two bearing sizes-- and backfilled with glue and foam. The phantoms were coated with clear latex paint to increase strength and resist flaking.

As an initial validation, we constructed a custom experimental rig to apply prescribed rotations to the bone phantom while being imaged under biplane fluoroscopy (Figure 1). The phantom was attached to a wooden U-shaped arm, which was in turn attached to a precision stage. A rotational potentiometer [6015 Rotary Series Precision Position Potentiometer, TE Connectivity, Schaffhausen, Switzerland] mounted in-line with the stage provided the gold-standard reference.

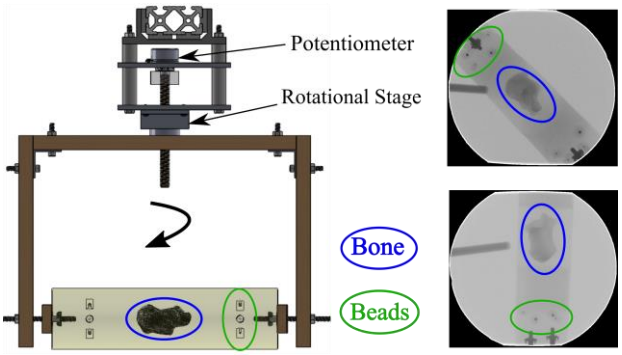


**Figure 1**: (a) Bone phantom attached to rotational mount, (b) Images of bone phantom under fluoroscopy

For each phantom, we first collected a battery of static poses at 0, 0.2, 0.4, 0.6, 0.8, 1, 2, 3, 4, 5, 7, 10, 15, 20, 25, 30, 35, and 40 degrees from the initial position. The phantom was aligned such that the rotation axis was normal to the bone's sagittal plane. Three dynamic rotation trials were then collected at approximately 5 degrees/sec. This procedure was then repeated with the rotational axis oriented normally to the transverse plane. Phantoms were positioned such that at least 3 markers were in view during the entire acquisition.

The biplane images were passed through a custom software pipeline to track bead coordinates; a screw axis decomposition was then used to calculate the rotation. This was compared to the potentiometer rotation to establish error.

## RESULTS AND DISCUSSION

Eight total bone phantoms (two calcanei, three tali, two first metatarsals, and one second metatarsal) have been constructed. Beads for one phantom have been tracked in both the sagittal and transverse view. The root-mean-squared (RMS) error for sagittal view was 0.23 degrees and the dynamic RMS errors were 0.08, 0.23, and 0.19 degrees. The RMS error for transverse view was 0.22 degrees and the dynamic RMS errors were 0.25, 0.13, and 0.49 degrees. These errors are consistent with results from our previous work.

**REFERENCES**
1. Miranda DL, Crisco JJ, J. of Biomech Eng, 2011, 133.
2. Iaquinto JM, et al., Computers in Biology and Med, 2018.

**ACKNOWLEDGEMENTS**
David Bennett of Diagnostic Imaging Services, National Institutes of Health, NIAMS AR069283

**Table 1:** Rotation error derived from comparison of potentiometer position to tracked bead position

| Error (deg) | Position (deg) | | | | | | | | | | | | | | | | | |
|---|---|---|---|---|---|---|---|---|---|---|---|---|---|---|---|---|---|---|
| | **0.0** | **0.2** | **0.4** | **0.6** | **0.8** | **1.0** | **2.0** | **3.0** | **4.0** | **5.0** | **7.0** | **10.0** | **15.0** | **20.0** | **25.0** | **30.0** | **35.0** | **40.0** |
| **Sag.** | -0.02 | -0.13 | -0.02 | -0.07 | -0.06 | 0.01 | 0.0 | -0.03 | -0.11 | -0.07 | -0.08 | 0.06 | -0.10 | -0.33 | -0.43 | -0.49 | -0.56 | -0.36 |
| **Tran.** | 0.01 | -0.12 | -0.04 | -0.04 | -0.10 | -0.03 | -0.10 | 0.10 | -0.05 | 0.05 | 0.15 | 0.24 | -0.08 | -0.11 | -0.38 | -0.57 | -0.34 | -0.35 |

# FEASIBILITY OF USING THE HTC VIVE SYSTEM TO COLLECT KINEMATIC DATA

Spitzley, K., Trempy, K. and Karduna, A.
Orthopaedic Biomechanics Lab, Dept. of Human Physiology, University of Oregon, Eugene, OR USA
Email: kspitzle@uoregon.edu

## INTRODUCTION

Recent improvements in Virtual Reality (VR) technology have exciting implications for the research and rehabilitative sciences. Various modes of VR have been used successfully as intervention modalities in these settings with great success [1,2]. However, VR systems have not yet been used as a mode of kinematic data collection. The use of these systems for both intervention and collection has the potential to greatly lower cost and increase portability of motion capture. While previous studies have looked at using the HTC VIVE headset as a tracking method with little success, use of the handheld controllers has not yet been explored [3].

The aim of this study is to gather preliminary data to investigate the feasibility of using the HTC VIVE VR handheld controllers to collect position and orientation data. To do so, we will compare the VIVE VR sensors and Polhemus Liberty sensors. The Liberty system has been robustly validated for scientific data collection, we therefore feel comfortable using it as a gold standard for comparison.

## METHODS

The VR system was set up as dictated by the VIVE owner's manual. The lighthouses were mounted 6 m apart at a height of 2.1 m and connected by the sync cable. The headset was placed on a stable shelf within the calibrated space. The magnetic tracking system (Polhemus Liberty, Colchester, VT) transmitter was placed 0.5 m from the sensor. Both systems sampled at a rate of 120 Hz.

The VIVE controller and Liberty sensor were mounted on opposite ends of a rigid segment with a common central point of rotation. This segment was mounted to a stable surface with a pegboard setup dictating five angular positions at 0°, 20°, 50°, 70°, and 90°. The sensors were moved through fifty permutations of these angular targets. Both sensors were sampling at a rate of 120 Hz. Data were collected from both sensors simultaneously using a customized Unity program.

Helical axis calculations were used to quantify the angular change in position from trail to trial. Angular measurement error between the sensors was quantified as absolute value of the difference in helical angle measured by the Liberty sensor and the VIVE sensor in each trial. Additionally, an RMS calculation was used to quantify drift in the signal.

## RESULTS AND DISCUSSION

Helical angles between sensors were similar over the fifty rotations tested. Average helical angle measurement error between the two sensors was 0.2° ± 0.1° and the largest error was 0.5°. Errors were then broken down by degree of angular movement (Figure 1).

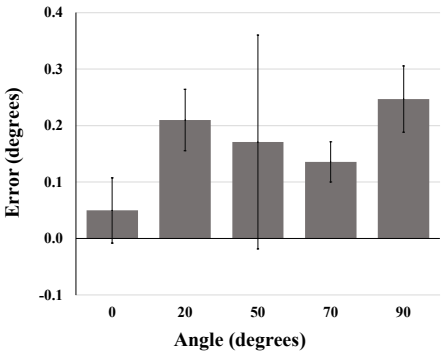


**Figure 1**: Difference in helical angle measurement between Liberty and VIVE sensors throughout a series of rotations to angular targets of 0°, 20°, 50°, 70°, and 90° (mean ± sd).

Average RMS over the ten trials did show some differences between sensors (Table 1). The VIVE demonstrated consistently higher measures of drift than the Liberty. However, both systems exhibited translational drift in the sub-millimeter range and rotational drift in the sub-degree range.

## CONCLUSIONS

While previous studies have used the VIVE headset as a tracking mechanism with little success, the handheld controllers are yet to be validated as a mode of data collection. Although the data presented here are preliminary in nature, they show promise for future measures of accuracy. It is our hope that with further validation, these controllers will be usable for kinematic data collection.

## REFERENCES

1. Rose, T., Nam, C., Chen, K. *Applied Ergonomics,* **69**, 153-161, 2018
2. Rodrigues Severiano, M., et al., *Arg Neuropsiquiatr,* **76**, 78-84, 2018
3. Niehorster, D., Li, L., Lappe, M., *i-Perception*, **8**, 1-23, 2018

**Table 1:** Average RMS drift of the position and orientation signals of the Liberty and VIVE systems.

| | Average RMS (mm) | | | Average RMS (degrees) | | |
|---|---|---|---|---|---|---|
| | **x** | **y** | **z** | **α** | **β** | **γ** |
| **Liberty** | 0.02 ± 0.02 | 0.03 ± 0.02 | 0.02 ± 0.01 | 0.00 ± 0.00 | 0.00 ± 0.00 | 0.00 ± 0.00 |
| **VIVE** | 0.61 ± 0.18 | 0.42 ± 0.12 | 0.60 ± 0.27 | 0.02 ± 0.02 | 0.01 ± 0.01 | 0.01 ± 0.0 |

# Muscle dynamics in jumping kangaroo rats (*D. deserti*)

Schwaner, M J [1], Lin, D C [2] and McGowan, C P [1, 3]
[1]Comparative Neuromuscular Biomechanics Lab, Department of Biological Sciences, University of Idaho, Moscow, ID USA
[2] School of Chemical Engineering and Bioengineering, Washington State University, Pullman, WA USA
[3]WWAMI Medical Education Program, Moscow, ID USA
e-mail: janneke.schwaner@gmail.com, web: http://www.webpages.uidaho.edu/McGowanLab/Research.htm

## INTRODUCTION

Kangaroo rats (family Heteromyidae) are bipedal hopping rodents that use erratic vertical jumps to escape their predators, mainly owls and snakes [1]. Previous research from our lab on the mechanics of these jumps indicates the ankle is the main contributor to net joint work when comparing across jump heights. In addition, we found that up to 30% of the net joint work, measured at the ankle joint with the use of an inverse dynamics analysis, is transferred from proximal muscles via biarticular ankle extensors. Given these results, the vastus lateralis (VL) muscle, a large knee extensor, and the lateral gastrocnemius (LG) muscle, a large ankle extensor, likely both play important roles in propelling the animal up during their vertical jumps. Therefore, we examined the in vivo performance of the LG and VL muscle during vertical jumping over a range of jump heights. We hypothesized that muscle shortening strain would be independent of jump height, but that relative electromyography (EMG) intensity would increase with increasing jump height.

## METHODS

Five adult, wild-caught desert kangaroo rats, *Dipodomys deserti*, were used for this study [body mass: 105 +/- 15 g]. The experimental set-up included a self-built plexiglass runway with a built-in force plate. Kangaroo rats were stimulated to jump off, of the force plate over an obstacle, which was changed in height every trial (0.1 – 0.5 meters). Sonomicrometry and EMG data were collected at 2000Hz. Jumping trials were recorded at 200 frames $s^{-1}$ using a high-speed camera (Xcitex Inc, Woburn, MA, USA), positioned perpendicular to the experimental set up. Video data were digitized using ProAnalyst (Xcitex Inc, Woburn, MA, USA), after which the complete dataset was analyzed using a customized analysis script for Matlab (2015a, MathWorks, Natick, MA, USA). Jump height was calculated using ballistic equations and force data.

## RESULTS and DISCUSSION

Out data suggests that our hypotheses are supported. There appears to be a linear relationship between jump height and relative EMG intensity for both the LG as well as the VL muscle, whereas net muscle shortening in both muscles does not change over increasing jump height.

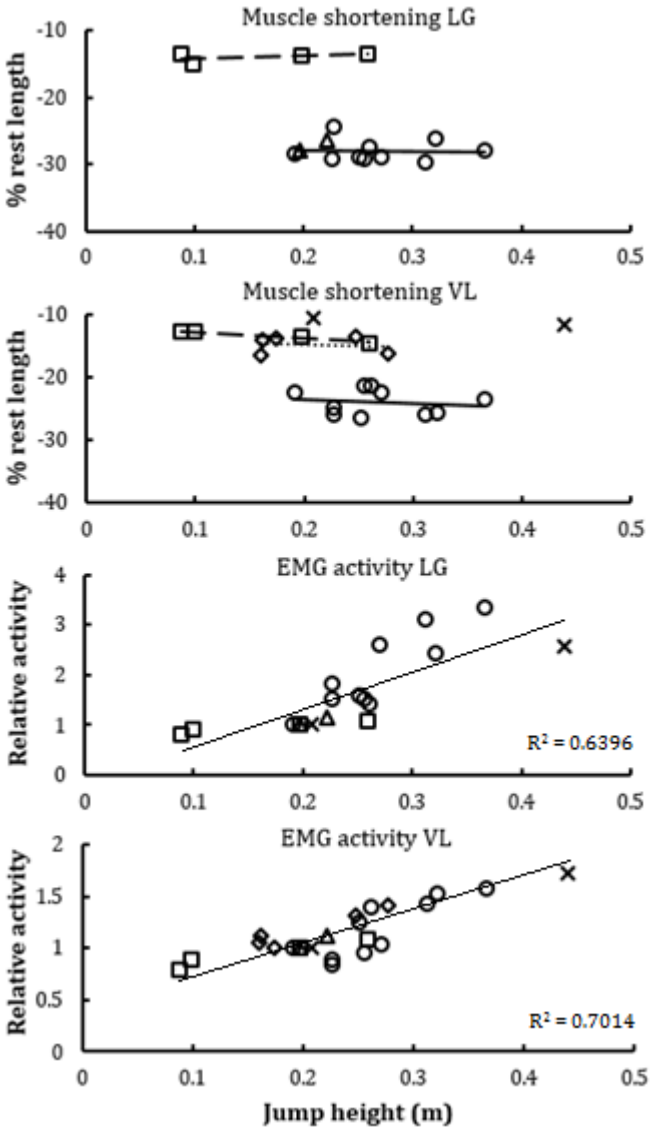


**Figure 1.** Muscle shortening (upper two graphs) and relative EMG activity (lower two graphs) of the lateral gastrocnemius (LG) and vastus lateralis (VL) muscle over jump height. Muscle shortening shows no change with increasing jump height in both muscles. Relative EMG activity (normalized against a common task of a 0.2 meter jump) does show a linear relationship with jump height. Every marker shape indicates a different individual.

## CONCLUSIONS

These results suggest that the increase in mechanical work required to achieve higher jumps is likely due to great muscle force and not due to greater length changes by the muscles.

## REFERENCES

1. Webster D & Webster M. *American Zoology* **20**, 247-254, 1980.

## ACKNOWLEDGEMENTS

The authors like to thank Dr JW Rankin for assisting with data analysis and providing feedback on the products of this research. This work was supported by NSF grant 1553550 (CPM) and ARO grant 66554-EG (CPM)

# In-Situ Contractile Properties of Kangaroo Rat plantarflexor Muscles

[1] Mehrdad Javidi, [2]Craig McGowan, and [1]David Lin
[1] Washington State University, Pullman, WA, USA
[2] University of Idaho, Moscow, ID, USA
Email: mehrdad.javidi@wsu.edu

## INTRODUCTION

The overall objective of our research study is to elucidate the mechanisms of extreme jumping performance in kangaroo rats (k-rats) by using forward dynamic simulations. The purpose of this study is to measure the *in situ* contractile properties of the plantarflexor group of three muscles (Medial Gastrocnemius (MG), Lateral Gastrocnemius (LG) and Plantaris (PL)) important for k-rat jumping. Measurement of the contractile properties includes the force-length (F-L) and force-velocity (F-V) relationships, which are integral to the muscle models used in forward dynamic simulations.

## METHODS

Six wild-caught k-rats (*Dipodomys Deserti*) (W=97.5±7.5 (gm)) were used in the experiments. Briefly, under deep anesthesia, the group of LG, MG, and PL were isolated, the sciatic nerve exposed for stimulation, and the femur fixed to mechanical ground. A bone chip connected to the distal part of Achilles tendon was removed from the calcaneus and attached to a servomotor (309C; Aurora Scientific, Aurora ON, Canada) used to control either force or position. Institutional approval was obtained prior to the experiments.

*Force-length (F-L) relationship:* To measure the F-L relationship, isometric forces were measured at seven different lengths of the muscle-tendon unit (MTU). Supramaximal activation was achieved with tetanic stimulation (3mA with 300 msec train of 0.2 msec biphasic pulses at 150 Hz) applied to the sciatic nerve. For each experiment, maximum isometric force ($F_{max}$) and optimum MTU length (MTUo) of muscle group were estimated from a 3rd order polynomial curve fitted to force vs MTU length. Maximum isometric stress, also was calculated as:

$$\sigma_{max} = (F_{max})/(PCSA) \quad (1)$$

where *PCSA* is the physiological cross section of area of all three muscles added together. *PCSA* of each muscle was calculated as:

$$PCSA^{muscle} = (m\cos(\beta))/(\rho\, L_{fiber}) \quad (2)$$

where, $m$, $\beta$, $\rho$ and $L_{fiber}$ are mass, pennation angle, density and fiber length of each muscle, respectively.

*Force-velocity (F-V):* Nine different isotonic forces within the range of $0.1F_{max}$ to $F_{max}$ were tested for each animal. For each isotonic force, the relaxed muscles were stretched to MTUo and isometric contraction obtained with a supramaximal stimulation. The servomotor then switched from length control to force control to induce isotonic shortening. Shortening velocity was the slope of the line which was fitted to MTU length data from 10 to 30 msec following initial force drop. To calculate maximum shortening velocity, force velocity data of each experiment was fitted with a hyperbolic curve (Hill's equation).

## RESULTS AND DISCUSSION

The scatter plot and fitted curve of pooled normalized active F-L data showed a clear maximum and ascending limb (Fig. 1A). Average maximum isometric force and maximum isometric stress were 24±1.7 (N) and 268±16 (kPa), respectively. Maximum isometric stress of the kangaroo rat ankle extensors was estimated by Biewener et al. to be 220-230 kPa [1], which appears to be consistent with our results.

The scatter plot and fitted curve of pooled normalized F-V data indicated that F-V curve of the muscle group was almost linear (Fig 1B). This linear relationship was different than the hyperbolic shape expected for the F-V relationship of a single muscle. Maximum shortening velocity of the muscle group was 1.23±0.05 (MTUo/sec).

## CONCLUSIONS

F-L and F-V relationships for the plantarflexor group of three muscles reflect the combined relationships of each single muscle. We are currently estimating the F-L and F-V relationships of each muscle from these data and additional measurements so that we are able to incorporate the experimental results in the forward dynamic simulation.

## REFERENCES

1. Andrew. A. Biewener, *et al.*, *J. exp. Biol*, **137**: 191–205, 1988.

## ACKNOWLEDGEMENTS

Funding provided by Army Research Office Grant #W911NF-15-1-0204 and NSF #1553550.

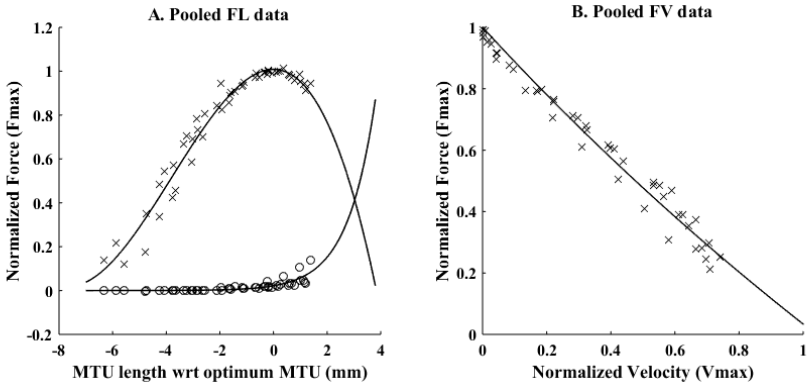


**Figure 1.** (A) Normalized active (×) and passive (o) F-L relationship. (B) Normalized F-V relationship.

# HIGH-STIFFNESS, MULTILAYERED GELATIN PHANTOMS FOR ULTRASOUND ELASTOGRAPHY VALIDATION

Lynda B. Brady,[1,2] Christina J. Stender,[2] and William R. Ledoux[1,2,3]
Departments of [1]Mechanical Engineering and [3]Orthopaedics & Sports Medicine, University of Washington, Seattle, WA USA
[2]RR&D Center for Limb Loss and MoBility, VA Puget Sound, Seattle, WA USA
email: lybrady@uw.edu

## INTRODUCTION

Ultrasound is a useful tool in the biomechanical study of soft tissues due to its unique ability to produce well-resolved images of internal soft tissues in real time. Further, the ultrasound technique shear wave elastography uses acoustic forces to calculate quasi-real-time tissue stiffness.[1] However, ultrasound imaging artifact is difficult to identify, and both ultrasound and shear wave elastography at large material strains like those experienced during gait is not well studied.

Study of large strain effects requires a stable phantom of known mechanical properties within the range of those found in the soft tissue of interest. Prior work on has focused on breast-mimicking gelatin and agar phantoms.[2] Adapting these phantoms for stiffer tissues with more realistic biomechanical properties is crucial for developing ultrasound protocols relevant to musculoskeletal soft tissues.

## METHODS

Constant gelatin concentration is necessary for stability in a multilayered phantom.[2] Therefore, a 10%wt gelatin phantom was used as a base to investigate the effects of additives on stiffness (Table 1). Gelatin (225 bloom, Sigma Aldrich) and agar (Sigma Aldrich) were saturated with distilled water and heated to clarification. For agar-gelatin phantoms, separate heated agar and gelatin solutions were added together and mixed for homogeneity. After a short cooling period, the crosslinker glyoxal (Sigma Aldrich) and/or preservative germall plus (99% diazolidinyl urea, 1% idopropynl butane), if used, were added and the solution was again mixed to homogeneity. Solutions were poured into molds and circulated on a shaker plate overnight to prevent separation during gelation and crosslinking. One-inch diameter discs were punched from the molded phantoms to match previous plantar soft tissue mechanical tests.[3] Phantoms were stored in safflower oil to prevent desiccation.

Discs were mechanically tested on an Electroforce 3200 mechanical testing machine (TA Instruments; New Castle, DE). Discs were preloaded to -0.2 N, then subjected to 3 cycles of 11 triangle waves at 2 and 0.5 Hz to 40% strain followed by a 0.75mm/s single triangle load-unload cycle to 50% strain, with a 4 minute rest period between cycles of triangle waves. Any damage sustained was recorded. Force and displacement data were post-processed in MATLAB (The MathWorks, Inc.; Natick, MA). Engineering stress and engineering strain were calculated. The elastic modulus was calculated as the slope from the middle of the stress-strain ramp curve to maximum stress and maximum strain.

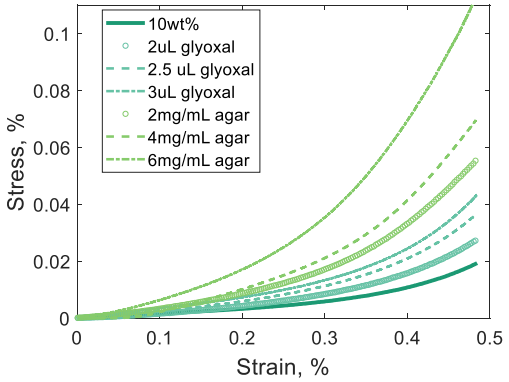


**Figure 1**: Preliminary results of mechanical testing.

## RESULTS AND DISCUSSION

The 10%wt gelatin-only phantom achieved stiffness of 75 kPa. Addition of the crosslinker gyloxal and preservative germall plus increased these stiffnesses by 20-100%. Addition of agar increased the stiffness of the phantoms by 172-445%. Phantoms were also tested for sonocompatibility with an Aixplorer® (Supersonic Imagine, Aixon-en-Provence, France), and were found to be visible at edges and largely transparent through homogenous regions at 14MHz.

Prior work indicates that plantar soft tissue has a modulus of 500 kPa-700 kPa in a healthy population and up to 1200 kPa in a diabetic population.[3] The stiffnesses presented here are below those of plantar soft tissue. However, the increased stiffness range of glyoxal and agar phantoms relative to the base gelatin phantom is promising. Higher gelatin base concentration, and increased agar or glyoxal concentration will likely increase the phantom stiffness into the range needed for biomechanically realistic plantar soft tissue. Scatterers such as glass beads or graphite could also increase material modulus in addition to improving sonocompatibility.

## REFERENCES

1. Bercoff et al. IEEE Trans Ultrason Ferroelectr Freq Control. (2004). 51(4): 396-409.
2. Madsen et al. Phys. Med. Biol. (2005). 50(23): 5597-5618.
3. Pai et al. J. Biomech. (2010) 43(9):1754:1760.

**Table 1:** Gelatin and agar concentration ratios.

| | | | | | | | |
|---|---|---|---|---|---|---|---|
| **Agar (wt%)** | 0 | 0 | 0 | 0 | 2 | 4 | 6 |
| **Glyoxal (uL)** | 0 | 2 | 2.5 | 3 | 0 | 0 | 0 |
| **Germall plus (mg)** | 0 | 121.6 | 121.6 | 121.6 | 6 | 6 | 6 |
| **Elastic Modulus (kPa)** | 75.3 | 91.5 | 130.9 | 151.7 | 205.2 | 270.0 | 410.9 |

# Design and characterization of stimulus intensity for a novel cam-follower vibrotactile actuator

Palve, L[1,2] and Rombokas, E[1,2]
[1]Department of Mechanical Engineering, University of Washington, Seattle, WA USA
[2]Center For Limb Loss and MoBility (CLiMB), Department of Veterans Affairs, Seattle, WA USA
email: lalitp@uw.edu, rombokas@uw.edu

## INTRODUCTION

Though there have been many designs for haptic feedback devices, there are still opportunities for improvement. In this paper, we present a vibrotactile actuator design that addresses four of these opportunities at once: 1) the capability to vary the frequency of stimulation while keeping amplitude constant 2) small contact area on the skin, for providing pinpoint locality of stimulation, but also for packing many stimulators into a small area 3) a novel means of providing constant loading (normal force pressing the tactor against the skin) 4) capability to customize the waveform of stimulation.

We demonstrate that stimulation with increasing amplitude, and independently with increasing frequency, results in increased subjective intensity on the thigh. The thigh is an interesting target because it is one of the least sensitive areas of the skin but is a natural target for stimulation by a lower-limb sensory feedback prosthesis. The effects as we vary amplitude and frequency appear consistent with those previously observed for hand.

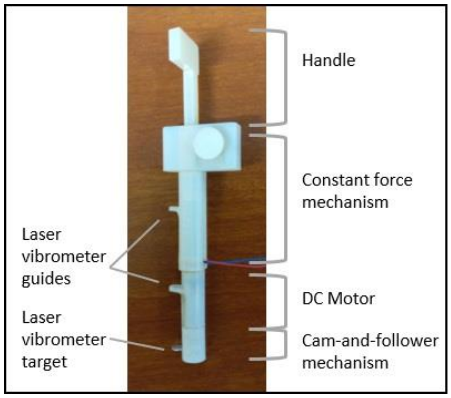


**Figure 1:** Cam-follower vibrotactile actuator with constant skin loading mechanism

## DESIGN AND EXPERIMENT

The device is based on a cam-and-follower mechanism attached to a DC motor and a constant force spring that keeps the loading on the skin constant.

Ten subjects (ages 22-28) were asked to sit in a chair while wearing noise-canceling headphones and a blindfold to prevent audio and visual cues. A site on their thigh, 5cm proximal from the knee, was stimulated randomly by one of four tactors (Figure 1.) Each tactor stimulated the skin at an amplitude of 100 µm, 200 µm, 330 µm or 580 µm. Each tactor stimulation frequency was also randomly driven at one of 128 Hz, 200 Hz and 278 Hz, all in the perceivable range of hairy and glabrous skin [2]. Tactor amplitude and frequency were randomized by block and the same number of presentations were used for each condition.

## RESULTS AND DISCUSSION

The stimuli were perceivable for all the experimental conditions. Figure 2, above, depicts the average perceived intensity for each amplitude of stimulation, averaged across all participants and frequencies. Perceived stimulation intensity increased with increased amplitude. Figure 2, below, depicts the effect of frequency. The differences in the means, ranging from around 1 up to around 7 for different displacement but only from around 4 up to 5 for frequency, suggests that changes in amplitude made a more profound difference than changes in frequency.

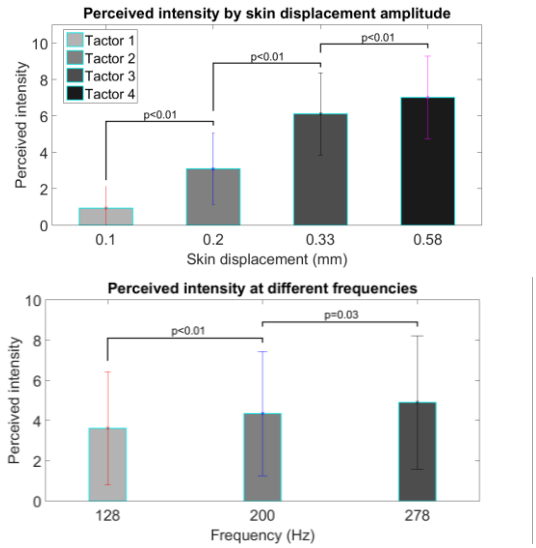


**Figure 2**: Perceived intensity for different amplitudes (above) and frequencies (below.)

We are now developing dense arrays of these vibrotactors for use in rich sensory feedback applications, e.g. facial tactile stimulation integrated with virtual reality (Fig. 3)

**Figure 3:** Facial tactile stimulation concept

## REFERENCES

1. Azadi M, and Jones L. "Vibrotactile actuators: Effect of load and body site on performance." In: *IEEE Haptics symposium*, Houston, United States, February 2014,
2. Wentink, E. et al. "Vibrotactile stimulation of the upper leg: Effects of location, stimulation method and habituation." In: Proc. Annu. Int. Conf. IEEE Eng. Med. Biol. Soc. 1668-1671 (2011).

# VALIDATION OF MICRO SPIKES FOR MOUNTING AN IMPLANT TO A TENDON

Won Suk You, Justin Casebier and Ravi Balasubramanian
Oregon State University, Corvallis, OR, USA
email: ravi.balasubramanian@oregonstate.edu, web: http://web.engr.oregonstate.edu/~balasubr/

## INTRODUCTION

In previous work, we have shown that it is biomechanically beneficial to use implantable passive mechanisms to re-engineer the mechanics of force and movement transmission within the body [1]. Overall, the new implant-based surgery provides increased finger flexion over the conventional surgery during physical-interaction tasks such as the grasping of objects.

The current embodiment of this implant requires the tendons to be sutured to the implant. It has been seen in an avian animal model that the suture creates too much trauma to the tendon, which then instigates a fibrotic healing response and long-term scarring [2]. This paper seeks to re-design the implant so that sutures are not necessary for long term adhesion. This paper presents preliminary designs of the implant, attachment method using micro spikes, and its durability via cycle testing.

## METHODS

The key requirement of the new implant design is to secure the implant to the tendon using a method that will promote secure attachment while mitigating foreign body response. To achieve this, two implant designs were made (Figure 1). Both designs use multiple micro spikes and sits between the tendons. After a survey of prior work that designed spikes for attaching implants to tendons, we chose the following spike dimensions: 275um base radius (R), 930um spike length ($L_s$), and 20° inclination from x-y plane. The spikes are angled toward the center of the implant to secure the tendon to the implant. Two samples of each 3D-printed implant were attached to the extensor digitorum longus in chicken cadavers approximately 8.5 mm distal of the natural bifurcation (one implant per leg). (Figure 2). Surgeries were performed by Dr. Jennifer J. Warnock, DVM (Oregon State University, College of Veterinary Medicine).

The implant's endurance in mechanically attaching to the tendon is validated by cycling the implanted legs as in Figure 4. Each leg was cycled for a total of 5000 cycles. The cycles were split up as follows: The first 2000 cycles were pulled with a force of 8N. This is the force required to fully extend a chicken foot under no load [3]. Next, the tendon is pulled with 11~12N for 2000 cycle to see how the implant and micro spikes endure a force higher than natural full extension. Finally, a 20N force is applied to the tendon for 1000 cycle to see whether it can withstand the extreme force. After conducting the cycle test, tendons and implants were dissected from the chicken legs and checked visually for any signs of wear or damage.

## RESULTS AND DISCUSSION

Figure 5 shows small marks on the tendon which signifies the micro spikes engaged mechanically with the tendon. Tissue residuals were also found on the spikes. Although some spikes showed wear, all the spikes survived the 5000 cycles.

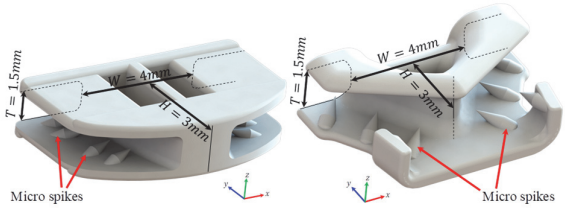


(a) Strut implant (b) V-shape implant

**Figure 1**: New implant design use either (a) micro spikes, or (b) both micro spikes and structural locking method to secure the tendon to the implant.

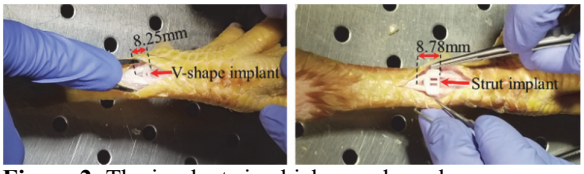


**Figure 2**: The implants in chicken cadaver legs.

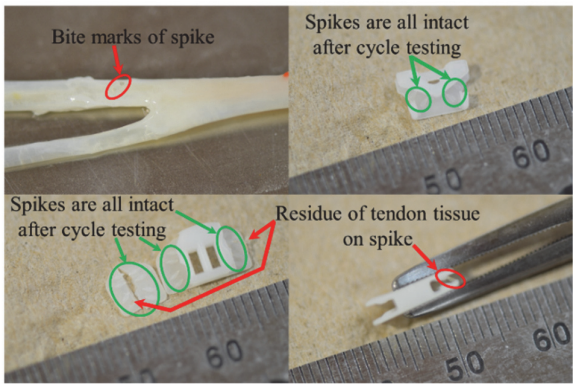


**Figure 3**: Tendon and implants after cycling test.

## CONCLUSIONS

In this paper, we presented designs of the implant, attachment method using micro spikes, and its durability via cycle testing. With the result of the cycling test, we conclude the micro spikes enable a secure mechanical attachment between biological tendon and implant. Future work includes validating the spike-based implants in vivo.

## REFERENCES

1. Homayouni et al. *IEEE Transactions on Biomedical Engineering*, **62**(9), 2208-2214, 2015.
2. Le et al. *Proceedings of 44th VOS Conference*, Snowbird, Utah, 2017.
3. Gilbert et al. *Journal of biomedical materials research*. **19**(5), 601-605, 1985.

## ACKNOWLEDGEMENTS

This work was supported in part by the CDMRP. Opinions, interpretations, conclusions and recommendations are those of the author and are not necessarily endorsed by the Department of Defense.

# PREDICTIVE MODELING OF HUMAN KINEMATIC RESPONSE TO ANKLE ORTHOSES DURING WALKING

Rosenberg, M.C.[1], Banjanin, B.[2] Burden, S.[2] and Steele K.M.[1]
[1] Department of Mechanical Engineering, University of Washington, Seattle, WA, USA
[2] Department of Electrical Engineering, University of Washington, Seattle, WA, USA
email: mcrosenb@uw.edu, web: https://depts.washington.edu/uwsteele/

## INTRODUCTION

Accurately predicting how individuals will respond to variations in ankle foot orthosis (AFO) mechanical properties, such as dorsiflexion stiffness or torque profile may be useful to inform clinical AFO prescription for individuals with motor impairments. Even with valid musculoskeletal models, predicting human locomotor response to AFO properties is challenging due to a lack of subject-specific models of neuromuscular control. Heterogeneity in physiology and motor control – particularly in clinical populations – may hinder the utility of population average-based models of motor control [1,2], motivating the use of a modeling framework that in not constrained by population-based assumptions. A data-driven modeling approach may be able to combine subject-specific neuromuscular and musculoskeletal information into a non-physiological model of how individuals' gait kinematics respond to AFO mechanical properties.

We developed a data-driven modeling paradigm to map between two points in the gait cycle using experimental data from walking with different AFO dorsiflexion stiffness levels (Figure 1). We expected that the model would predict of gait response to new AFO stiffness levels with comparable accuracy to in similar non-AFO studies of gait.

## METHODS

We collected kinematic data (Qualisys, Goteborg, SE) from one unimpaired adult (female, age=27, height=173cm, weight=63.5kg) walking at a self-selected speed (v=1.3 m/s) on a treadmill with bilateral AFOs. The participant walked for four minutes per trial under four stiffness conditions ($k_0$=0, $k_1$=4203, $k_2$=7530, $k_3$=9807 N/m). Marker trajectories were low-pass filtered at 6 Hz using a 4th order Butterworth filter. We estimated AFO torque using a linear spring force-strain relation and AFO geometry.

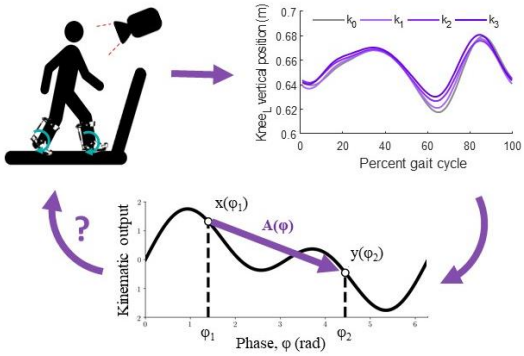


**Figure 1**: The modeling paradigm takes kinematic data from walking at multiple AFO stiffness levels, fits a map $A(\varphi)$ between to gait phases, and attempts to predict kinematics for walking at a new AFO stiffness level.

We generated the phase-varying model by estimating a kinematic phase of each gait cycle [3], then fitting a phase-varying linear map, $A(\varphi)$, between kinematic data at an initial phase, $\varphi_1$, and data at future phases, $\varphi_2$, where $\varphi_2 = \varphi_1 + \Delta\varphi$, and $\Delta\varphi$ is a lookahead window (Figure 1). This yielded a model of the form $y(\varphi_1+\Delta\varphi)=A(\varphi)x(\varphi_1)$ [4]. The input states, $x(\varphi_1)$, consisted of AFO torque profiles, all lower-limb and torso kinematic markers trajectories and their derivatives. Output states, $y(\varphi_2)$, consisted of sagittal-plane pelvis (ASIS, PSIS markers), lateral knee and ankle markers, and foot positions (5th metatarsal marker). The model was trained using data from $k_0$, $k_1$ & $k_3$ trials, and tested using data from the $k_2$ trial. We evaluated model quality using relative remaining variance (RRV), which quantifies a model's ability to reconstruct measured signals.

## RESULTS AND DISCUSSION

ASIS and PSIS trajectories were well predicted in the fore/aft and vertical directions (Figure 2, RRV<13%). These results used a fixed lookahead window of π/2, or roughly 25% of the gait cycle, and generate maps by propagating the initial state over the gait cycle. Lower limb motion was not as well predicted in the fore-aft direction (RRV<22%), though these RRV values were lower than those in a similar study of human running [4]. Furthermore, as we tested on the middle stiffness level, these results suggest that the proposed modeling framework may enable useful predictions of gait from untested AFO torque profiles by experimentally capturing only the extrema of a range of AFO mechanical properties.

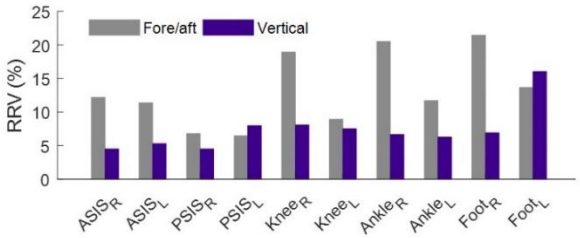


**Figure 2**: Average relative remaining variances (RRVs) suggest that the model accurately predicted most states. RRV values close to zero indicate a more accurate prediction. Subscripts *R* & *L* denote right and left legs, respectively.

## CONCLUSIONS

This study found that an abstract, phase-varying model had the potential to predict changes gait with AFOs. Refinement of this framework may inform clinical AFO prescription and enhance outcomes of AFO interventions for individuals with motor impairments.

## REFERENCES

1. Steele KM, et al. *Dev Med & Child Neurology*, **57**, 1176-1182, 2015.
2. Handsfield GG, et al. *Musc & Nerve*, **53**, 933-945. 2016.
3. Revzen S & Guckenheimer J. *Phys Rev E* **78**, 2008.
4. Maus HM, et al. *J R Soc Interface*, **12**, 2014.

## ACKNOWLEDGEMENTS

This work was supported by a National Science Foundation Grant CBET-14526 and a Graduate Research Fellowship, and University of Washington AMP Lab & College of Engineering Strategic Research Initiative (SRI).

# Development of an Omnidirectional Neck for Evaluation of Protective Equipment

Fonseca, G., Whyte, T., and Cripton, P.A.
OIBG, Dept. of Biomedical/Mechanical Engineering, University of British Columbia, Vancouver, BC Canada
e-mail: gfonse01@mail.ubc.ca

## MOTIVATION

There are an estimated 12.5 million people worldwide living with a spinal cord injury (SCI) [1,2]. The most common injury is to the cervical spine [3]. The population suffering from a traumatic brain injury (TBI) is an equally staggering number, with approximately 10 million people affected each year [4]. SCIs and TBIs are most often due to vehicle collisions, falls and sports related impacts, respectively [1,3].

## INTRODUCTION

Safety devices meant to protect the head and neck in transportation, occupational and sports settings can be tested and evaluated with the use of an anthropometric test device (ATD). The Hybrid III neck is the most commonly used surrogate as it is specified in automotive and helmet standards, however, the Hybrid III neck is only biofidelic in high speed rear or frontal vehicle collisions [5,6,7,8]. There is currently no single surrogate appropriate for complex, multiple plane loading that often occurs in real world head impacts or inertial loading [9]. For this reason, various designs are used to simulate the response of the healthy human neck, dependant on the location and direction of impact, acceleration and/or velocity.

The long-term project objective is to create a singular surrogate biofidelic omnidirectional neck for head first impacts, head impacts in the transverse plane and inertial loading, as in motor vehicle collisions, during three levels of preparedness; asleep, awake and not braced, and awake and braced. The goal of this research, a first step towards the overall objective, is to reproduce kinetic and kinematic responses of sub-axial functional spinal units (two or more vertebrae and the intervertebral discs between them) of a "sleeping," individual (by this we mean a passive spine with no need to simulate more than passive muscle properties).

## PROPOSED METHODS

The first phase will be to model sub-axial cervical vertebrae after healthy 50$^{th}$ percentile adult male and female at 40, 14 and 8 years of age. Modelling the sub-axial vertebrae after human anatomy was a calculated choice. Understanding the characteristics of a functional spinal unit (FSU) is believed to be the key to understanding the kinetics and kinematics of the sub-axial cervical spine in its entirety [10]. Additionally, the mobility of the neck is defined by its geometry. The overall natural curvature of the cervical spine provides stability and the individual vertebral geometry defines the range of motion [11]. By incorporating the geometry of healthy vertebrae into the design, it is hoped that a biofidelic omnidirectional range of motion will be achieved.

We will obtain CT scans of healthy cervical vertebrae. The axial scans will be used to 3D print metal vertebrae. The choice of metal was based on Dr. Nelson's repeatable and durable biofidelic surrogate neck design that was constructed previously in our laboratory using aluminum vertebrae.

The next step will be to construct the functional spinal unit. Accurate disc material is crucial to this step. Disc compression and viscoelasticity leads to a biofidelic range of motion as well as a lag in force development in the upper and lower neck in axial loading to the spine, resulting from head first impacts [9,11]. The material for the discs will be selected/created after studying the mechanical properties of the disc's nucleus pulposus (inner core) and the annulus fibrosus (outer ring). Although muscles do not need to be incorporated in the "sleeping," model of an FSU, surrogate ligaments are still required and will be attached to the vertebrae.

Tension-compression, flexion-extension, lateral bending and axial rotation tests will be carried out in our laboratory and the motion will be analyzed by a motional analysis system. The kinetic and kinematic results will be compared to data from published studies and testing previously performed in our laboratory, specifically the stiffness matrices we have created, to assess biofidelity.

## CONCLUSIONS

Reproducing the kinetic and kinematic responses of sub-axial functional spinal units will aid in the construction of a surrogate biofidelic omnidirectional neck. The ultimate goal is to use the surrogate neck to improve safety equipment meant to protect the head and neck in transportation, occupational and sports settings.

## REFERENCES

1. Cripps RA, et al. *Spinal Cord* **49(4)**, 493–501, 2011.
2. WHO. *Spinal Cord Injury.* Retrieved from http://www.who.int/mediacentre/factsheets/fs384/en/
3. Singh A, et al. *Clin. Epidemiol.* **6**, 309–331, 2014.
4. Humphreys I, et al. *Clinicoeconomics & Outcomes Research* **5**, 281–287, 2013.
5. Foster JK, et al. *Proc of the 21st Stapp Car Crash Conference,* New Orleans, Lousiana, 1977.
6. Nightingale RW, et al. *Proc 35th Stapp Car Crash Conf, Society of Automotive Engineers,* San Diego, California, 1991.
7. Gwin JT, et al. *J. Biomech. Eng.* **132,** 011006–9, 2010.
8. Fréchède B, et al. *Ann Biomed Eng.* **37**,1403–1414, 2009.
9. Nelson TS, et al. *Traffic Inj Prev* **11(3):**309–319, 2010.
10. Stokes IAF, et al. *J. Biomech.* **34**, 733–740, 2001.
11. Drake RL, et al. *Gray's Basic Anatomy.* Elsevier, 2012

## ACKNOWLEDGEMENTS

I would like to thank Dr. Brian Kwon for his support in CT scan retrieval and ICORD and OIBG for the use of their facilities.

# *Ex vivo* evaluation of intervertebral disc mechanics using diffusion imaging on the 7T MR: effect of degeneration

McGivern, K, Yung, A, Cripton, P and Wilson, D
ICORD - Orthopaedic and Injury Biomechanics Group, University of British Columbia, BC, Canada
Centre for Hip Health and Mobility (CHHM), University of British Columbia, BC, Canada
Email: Kelsey.mcgivern@gmail.com

## INTRODUCTION

Degenerative disc disease is a prevalent problem, espeically for the aging population. Degenerative discs are found in 10% of people aged 20-29, and increases with age to 96% in those over 60 years old [1].

When looking at intervertebral disc (IVD) degeneration, there has been a major challenge in differentiating changes that occur solely due to ageing from those that might be considered pathological; uncertainty still exists regarding the exact anatomic and physiologic basis for several clinical symptoms [2]. There is a need to understand the effect of degeneration on the mechanical behaviour of the disc, which may be a better indicator of clinical symptoms than simply anatomic changes.

T2-weighted imaging in MRI is used extensively for grading degeneration of the IVD. The Pfirrmann grade can effectively describe anatomic variations and morphologic changes [3]. However, Pfirrmann grade is unable to distinguish painful discs from asymptomatic ones.

Diffusion imaging, an MR technique, has strong potential for assessing the mechanics of the IVD and disruption of these mechanics due to pathology. It has recently been shown that MR diffusion measurements are sensitive to different loading conditions [4], a property not evident on a conventional T2-weighted MRI scan. However, the loading conditions in this previous study only considered two neutral postures of the spine: supine and standing. It is still unknown how bending moments caused by flexion and extension affect MR diffusion measurements in both healthy and degenerated discs.

## OBJECTIVES

- 1: Develop a protocol for measuring the Apparent Diffusion Coefficient (ADC) in the intervertebral disc using diffusion imaging on the 7 T MR scanner
- 2: Determine the relationship between ADC values and simulated physiological load (flexion, extension, and upright standing) applied to both healthy and degenerated disc
- **Future aim**: Extend the developed methods to the upright open 0.5 T MRI in order to assess the feasibility of using the established protocol to evaluate disc mechanics *in vivo*

## METHODS

Pilot testing has been performed to establish a diffusion-weighted imaging sequence on a Bruker Biospec 70/30 7.0 Tesla MRI scanner. The parameters for this sequence were chosen to establish a good balance of diffusion weighting, contrast between different anatomic regions of the disc, and a reasonable scan time of 1 hour or less. **Figure 1** shows a resultant ADC map obtained using this sequence.

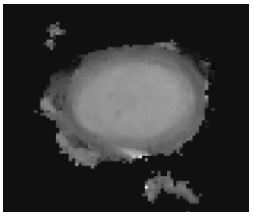

**Figure 1** – Resultant ADC map showing axial slice of a bovine FSU

Two groups of specimens will be tested. For both groups, human functional spinal units (FSUs) will be used at the L4/L5 and L5/S1 levels, as these two levels are the largest discs in the human body, with the largest degree of flexion and extension in the lumbar region, and finally is the most common site of LBP clinical presentation [5].

FSUs will be placed within an MR compatible rig that is able to apply both compressive and bending loads to the FSU. FSUs will be imaged under 6 different loading conditions which simulate flexion, extension and neutral standing postures.

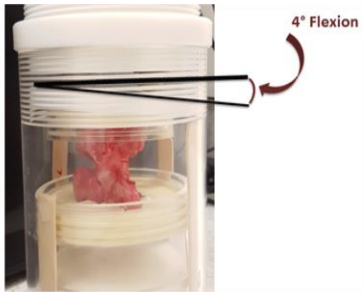


**Figure 2** – Bovine FSU in MR-compatible rig under simulated flexion posture

A group of healthy discs (Pfirrmann grade I-II) will be imaged to establish the expected changes to ADC values under simulated physiological loading. Next, a group of more severely degenerated discs (Pfirmann grade IV-V) will be imaged following the same protocol.

### Potential Impact

The study will shed light on the effects of bending moments to MR diffusion measurements under simulated physiological loading conditions. Further, this will allow direct assessment of how degeneration affects ADC measurements in the disc, which may provide insight into subtle changes in mechanical behaviour of the disc as degeneration progresses.

## REFERENCES

[1] J. S. Lawrence, *Ann. Rheum Dis.*, vol. 11, no. 2, pp. 121-138, 1969
[2] J. Takatalo *et al.*, *Spine*, vol. 36, no. 25, pp. 2180–2189, 2011.
[3] C. W. Pfirrmann *et al.*, *Spine*, vol. 26, no. 17, pp. 1873–1878, 2001.
[4] R. Alkalay, *Integrated Biomaterials Science*, pp. 403–424, 2015.
[5] E. I. T. de Schepper *et al.*, *Spine*, vol. 35, no. 5, pp. 531-536, 2010.

# Age and Gender Effects on Hybrid III ATD Lumbar Spine Failure Loads

Sean Maroney[1,2] and Sean D. Shimada, Ph.D.[1]
[1]Biomechanical Consultants, Davis, CA USA
[2]Sacramento City College Sacramento, CA USA
Email: seamaroney@ucdavis.edu

## INTRODUCTION

The Hybrid III Anthropomorphic Test Device (ATD) family is currently used for automotive accident research and testing to determine the potential for injury in human occupants. The 50th percentile male Hybrid III ATD, in part, was based upon the anthropometric characteristics from a 49-year-old male volunteer [1]. Subsequent to its development, the 50th percentile male ATD was scaled using the Mertz method to create the Hybrid III family which includes the 5th, 50th, and 95th percentile male and female devices [2]. The scaling procedure for the Hybrid III ATD family assumes the soft tissue properties such as range of motion and force producing/resisting capabilities are constant regardless of age and gender. However, the current literature suggests that muscle and ligament mechanical properties begin to degrade as one ages, decreasing their force producing/resisting capabilities [3,4]. Furthermore, it has also been demonstrated that soft tissue characteristics differ between males and females, which also biomechanically differ between genders as they age [5]. Over the course of a lifetime, a reduction in muscle and ligament strength leads to changes that impact injury tolerances. In order to increase the biofidelity of ATDs, factors such as age and gender need to be taken into account. This study proposes to scale the 50th percentile male ATD to various sizes while accounting for changes due to age and gender. The proposed model would be used to more accurately represent the shear failure loads of the lumbar spine defined in the literature.

## METHODS

The anthropometric data for the standard 50th percentile male Hybrid III ATD was retrieved from the National Highway Traffic Safety Administration (NHTSA) database. The Mertz scaling method was implemented to account for individuals of differing sizes [2]. Lumbar shear force characteristics were found for the 50th percentile male Hybrid III ATD and several male cadavers in Begeman, et al. [6]. Additionally, data associated with lumbar spine muscle and ligament strengths, specific to age and gender traits, were compiled through a comprehensive literature search. The data was compiled and analyzed using a regression analysis to determine trends in the individual soft tissue properties. The resulting regression coefficients from the analyses, in conjunction with the Mertz scaling method [2], allowed us to redefine the lumbar shear responses specific to gender, age, height, and weight.

## RESULTS AND DISCUSSION

After the regressions were determined for the effects of age and gender on muscle and ligament strength in the lumbar spine, the failure loads from the Hybrid III ATD from Begeman, et al. [6] were scaled to more accurately describe the changes in soft tissue properties each gender experiences over the course of a lifetime. Both the posterior and anterior shear failure loads were determined for use in rear and frontal impact scenarios, respectively. The application of the regression coefficients to the anterior and posterior shear characteristics of the 50th percentile male Hybrid revealed that the lumbar shear tolerances decreased for both male and females as they age. In Figure 1, the Begeman, et al [6] 50th percentile male Hybrid III posterior shear failure load is compared to the male and female 50th percentile posterior failure shear load when scaled to age and gender.

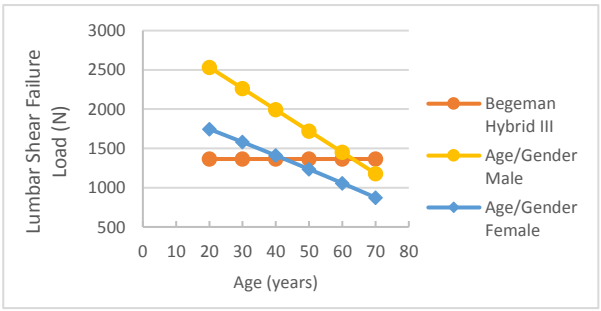


**Figure 1: Comparison of Posterior Lumbar Shear Failure Loads for Pre-Scaled and Scaled Hybrid III ATD**

The figure demonstrates that male failure loads are consistently higher throughout their lifespan when compared to females; however, a female's rate of decrease in failure load is less over time when compared to males. This trend remains the same for the lumbar anterior shear failure loads.

## CONCLUSIONS

The differing rates of change in the shear failure loads indicate that while males may have stronger muscles and ligaments, females are better able to maintain their muscle mass and ligament strength as they age. By accounting for age and gender soft tissue characteristics in the lumbar spine of the Hybrid III ATD family, we believe the implementation of the proposed model will improve the accuracy of accident injury analysis.

## REFERENCES

1. Mertz, H. and Patrick, L., *Strength and Response of the Human Neck**, SAE Technical Paper 710855, 1971
2. Mertz, H. J., et al., *Size, Weight and Biomechanical Impact Response Requirements for Adult Size Small Female and Large Male Dummies*, SAE Technical Paper Series, 1989.
3. Ellis, Benjamin, et. al., *Effects of Aging on Cellular Function, Healing, and Mechanical Properties of Ligaments*, Engineering Materials and Processes (EMP), 2014.
4. Gao, Yingxin. *Mechanical Properties of Aging Skeletal Muscle*, Engineering Materials and Processes (EMP), 2014.
5. Kirchengast, Sylvia, et. al., *Gender and age differences in lean soft tissue mass and sarcopenia among healthy elderly*, 2009.
6. Begeman, P. C., et. al., *Viscoelastic Shear Responses of the Cadaver and Hybrid III Lumbar Spine*, SAE Technical Paper 942205, 1996.

# COMPARISON OF MENTAL IMAGERY AND UNILATERAL TRAINING ON MUSCULAR STRENGTH

van Rooyen, C., Burgess, E., Atwell-Scrivner, J., & Cannavan, D.
Exercise Science Laboratory, Dept. of Health and Human Performance, Seattle Pacific University, Seattle, WA USA
email: vanrooyenc@spu.edu

## INTRODUCTION

Throughout an individual's lifetime, it is not uncommon to suffer an injury, or fall victim to an illness, that results in immobilization of whole or part of one's body. While there are many ways to regain strength post-immobilization, there are fewer strategies used during the immobilization period.

Both mental imagery and unilateral training increase muscular strength through neurological adaptations and excitability. Indeed, researchers found that mental imagery and unilateral training can combat strength losses caused by injury and immobilization (Newsom et al., 2003; Pearce et al., 2012). A major aim of the rehabilitation process should be to prevent atrophy as this will ensure a faster return to the pre-injured condition. Therefore, the purpose of this study was to compare the effect of mental imagery and unilateral training on muscular strength in the biceps brachii.

## METHODS

Eighteen healthy, right handed, college students volunteered for the present study (age 21±1.2; height 70±3.1 in.; weight 158± 24.5 lbs). Participants warmed up via arm circles, swings, and weightless bicep curls. Upon completion, elbow flexor strength was assessed at $45^{o} \cdot s^{-1}$ using an isokinetic dynamometer (Biodex System 4 Pro) . Both left and right arms were assessed. Peak torque recorded over three repetitions was used for data analysis. . The Biodex lever arm attachment was set to move the participant's arm through 105° (just short of full extension to full flexion) to mimic the movement of a bicep curl.

The participants were randomly assigned to a mental imagery (n=9) or unilateral training group (n=9) for a four-week intervention. The mental imagery group imagined themselves performing a weighted bicep curl in first-person for five minutes a day, five days a week. The unilateral training group completed three sets of ten bicep curl repetitions on their right arm using an exercise band.

Statistics were analyzed using magnitude-based inference (MBI). MBI gives information regarding the size and direction of the effect in the format of a three-level scale of magnitude, (% +tive / %trivial / % -tive). Hopkins Chances spreadsheet and R script were used to calculate MBI (Batterham & Hopkins, 2006).

## RESULTS AND DISCUSSION

Results were categorized into within-group (Table 1) and between-group (Table 2) analysis. Mechanistic inferences were made from the percent probabilities using a chart that interprets ranges of probabilities into verbiage. All within-group comparisons were very likely trivial except for mental imagery with the right arm. Right-handed individuals could have a possible increase in strength in their right arm using mental imagery. Both between-group comparisons had possible beneficial effects using mental imagery compared to unilateral training in both the right and left arms.

While there are no guarantees for improvement, an individual undergoing rehabilitation might consider adding five minutes a day of mental imagery for possible neurological adaptations to maintain strength in their dominant side, which should also speed-up their return to pre-injury strength.

## REFERENCES

1. Batterham, A.M., et al. *International Journal of Sports Physiology and Performance*, *1*(1),50-57, 2006.
2. Newsom, J., et al. *Journal of Sport Rehabilitation*, *12*(3), 249-258, 2003.
3. Nyberg, L.,et al. *Neuropsychologia*, *44*(5),711-717, 2006.
4. Pearce, A.J., et al. *Scandinavian journal of medicine & science in sports*, *23*(6), 740-748, 2012.

**Table 1.** Within group comparisons for the change in strength (N·m).

| Group | Comparison | Diff ± 99% CI | Probability of the Effect (% +ive / % Trivial / % -tive) |
|---|---|---|---|
| Unilateral | Right Post - Pre | -0.355 | (0.4 / **98.3** / 1.3) |
| Unilateral | Left Post - Pre | -1.02 | (0.2 / **96.2** / 3.6) |
| Imagery | Right Post - Pre | 2.26 | (**34.9** / 64 / 1.1) |
| Imagery | Left Post - Pre | 0.87 | (3.8 / **95.9** / 0.3) |

**Table 2.** Difference in changes in strength (N·m) between the unilateral training and imagery groups.

| Diff ± 99% CI | Diff ± 99% CI | Probability of the Difference (% Unilateral > Imagery / % Trivial / % Imagery > Unilateral) |
|---|---|---|
| Uni R – Imagery R | -2.66 | (1.1 / 55.2 / **43.7**) |
| Uni L – Imagery L | -3.28 | (0.6 / 44.5 / **52.9**) |

# THE EFFECTS OF TIGHT HIP FLEXORS ON GAIT

Reid, K., Yngsdal, M., Atwell-Scrivner, J., & Cannavan, D.
Seattle Pacific University, Seattle, WA, USA
Email: reidk2@spu.edu

## INTRODUCTION

The hip is the center of movement in the body and high demands are imposed upon it during daily tasks. Hip joint injuries are common throughout life and a decrease or lack of mobility in the hip can increase fall risk in the elderly[1] and limit exercise performance. A lack of hip mobility may be caused by tight hip flexors. Tight hip flexors could alter gait patterns through a decrease in hip extension, this could also impair running performance.

Hip flexor range of motion is commonly tested using the Thomas test. Normal hip flexor extension would be observed with the thigh (hamstring muscle group) resting flat on a massage bed during the examination. Proprioceptive neuromuscular facilitation (PNF) stretching is commonly used by clinicians to increase both passive and active flexibility at the hip joint. Active flexibility is important for gait due to the active movements that a gait cycle requires[2].

There is limited research examining the effects of tight hip flexors on gait patterns in a young healthy adult population. Therefore, the purpose of this study was to examine the effects of PNF stretching, on adults with tight hip flexors, on gait parameters.

## METHODS

Nine healthy females (Mean ± SD; age: 21.6 ± 0.5y), free from musculoskeletal disorders, volunteered for this study. Research was conducted in the Exercise Science Laboratory at Seattle Pacific University.

A requirement to participant in the study was the presence of tight hip flexors. If a subject did not have tight hip flexors she was excused from the study. Data for each subject were collected in a single 30-minute session. Data were collected in the following manner: 1) Thomas test, 2) treadmill gait analysis at a self-selected speed that mimicked walking speed, and 3) a step and stride length test (using talcum powder on black butcher paper). After the initial evaluation, Hold-Relax PNF stretching occurred until a visual change in hip extension was observed. The stretching was conducted while the subject was in the Thomas Test position. Two repetitions of stretching on each leg occurred. Following the PNF stretching, the pre-stretch measurements were repeated to assess changes.

## RESULTS AND DISCUSSION

Data are still being collected and analyzed and the results are unavailable at present. Figure 1 and Figure 2 represent the Thomas test before and after PNF stretching occurred; note the increased range of motion of the hip flexors.

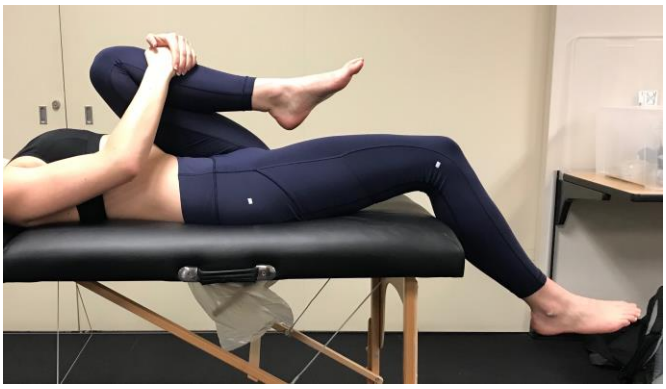

**Figure 1.** Hip flexor tightness pre PNF stretching

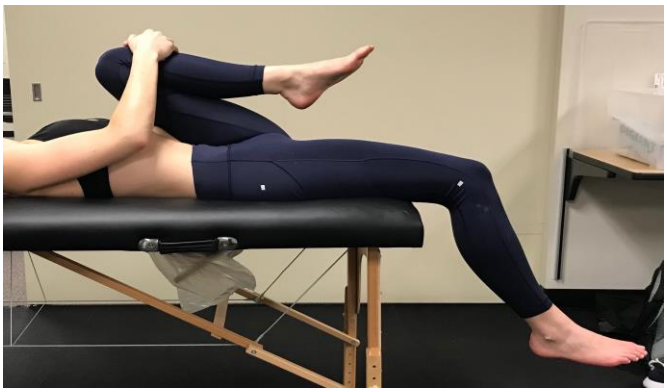

**Figure 2.** Hip flexor tightness post PNF stretching

## REFERENCES

1. Kerrigan, D.C., Lee, L.W., Collins, J.J., Riley, P.O. and Lipsitz, L.A., 2001. Reduced hip extension during walking: healthy elderly and fallers versus young adults. *Archives of physical medicine and rehabilitation*, *82*(1), pp.26-30.
2. Sharman, M.J., Cresswell, A.G. and Riek, S., 2006. Proprioceptive neuromuscular facilitation stretching. *Sports Medicine*, *36*(11), pp.929-939

# FLIP FLOPS AND BAREFOOT WALKING COMPARISON IN WOMEN AGES 18-25

Burgess, E., Atwell-Scriver, J. & Cannavan, D.
Seattle Pacific University, Seattle Pacific University, Seattle, WA, USA
email: burgesse@spu.edu

## INTRODUCTION

Heel pain, shin splints and generalized shank and foot pain have been attributed to prolonged use of flip flops[1]. Despite negative health consequences, flip flops continue to be a popular choice for female adults. Carl & Barrett found that in a United States shopping mall twice as many women wore flip flops compared to athletic shoes[2]. In addition, previous research has found that flip flops increase ankle dorsiflexion compared to other shod and unshod condition[3,4,5]. It has been hypothesized that the increased dorsiflexion helps keep the flip flop on[3]. At present, there is limited research investigating how flip flops modify walking in adult populations. Thus, the aim of the present study was to analyze the walking gait patterns of unshod (barefoot) walking gait and walking gait while wearing flip flops in healthy, female, college students, ages 18-25.

## METHODS

Seven university females with no health or injuries that affected gait participated in this study (Mean ± SD; age 21.14±0.64y; mass 61.9±4.9kg). Data were collected in the Exercise Science Laboratory at Seattle Pacific University. Upon completion of health screening and consent form signature, anthropomorphic measurements were recorded. The investigator measured height, weight, shoe size, and leg length. Anatomical markers were placed on the left leg. Specifically, markers were placed on the following: head of the fifth metatarsal, lateral malleolus, center of knee joint, and greater trochanter. An additional marker was placed on the right greater trochanter to measure leg length. Participants completed a 10-minute warm up walking barefoot (for 5-min) and then with flip flops (for 5-min) on a treadmill at a self-selected speed that mirrored typical walking speed. After a 5-min rest interval, participants were filmed walking for 5-min in both conditions (barefoot and flip flop conditions were randomized). There was a 5-min rest period between each condition. Recordings were made in the sagittal plane at 120 frames per second. Data were processed offline using Kinovea software (Figures 1-3). The following parameters were measured: 1) step and stride length, 2) swing and stance times and 3) cadence. In addition, degrees of dorsiflexion, knee flexion and hip flexion were recorded upon heel contact. Finally, joint angle at toe-off was recorded for plantarflexion, knee extension, and hip extension.

## RESULTS AND DISCUSSION

There were significant ($p$<0.05) increases in the following for the flip flops condition: step, stride, and stance time, and knee flexion at heel strike. Hip extension at toe-off and cadence significantly decreased in the flip flops condition compared with barefoot. Interestingly, unlike, previous research there was no significant ($p$>.05) difference in ankle dorsiflexion at heel strike between conditions. One individual transitioned from forefoot strike in barefoot, to heel strike when wearing flip flops.

The significant differences between walking in flips flops and barefoot could be due to altered proprioception feedback. For instance, the increased step and stride time in flip flops could be due to decreased proprioception at heel strike. At toe off, the flip flops may have provided increased sensory feedback as it dragged on the treadmill. Subsequently, increased knee flexion could be required to keep the flip flops in the correct position allowing foot clearance at toe-off. These changes in proprioceptive feedback may alter muscle recruitment strategies which may be the root cause of musculoskeletal issues associated with flip flops.

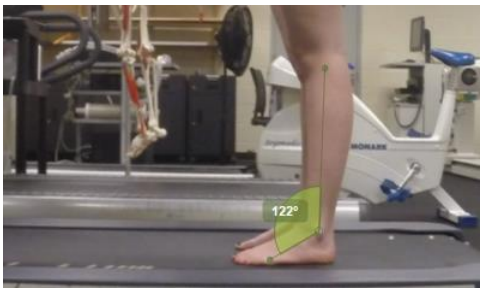


**Figure 1**: The angle of ankle while the participant is standing is considered 90°.

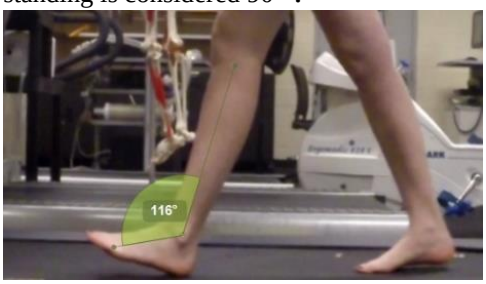


**Figure 2:** Using the reference angle from the subject standing, the angle of dorsiflexion at heel strike is 6° while unshod.


**Figure 3:** Using the reference angle from the subject standing, the angle of dorsiflexion at heel strike is 12° while wearing flip flops.

## REFERENCES

1. Popular Flip-flop Sandals Linked To Rising Youth Heel Pain Rate. *Am College Foot Ankle Surgeons*, 2007.
2. Carl TJ, et al. *J. Am Podiatr Med Assoc*, **98**, 374-378, 2008.
3. Chard A, et al. *J Foot Ankle Res*, **6**, 8, 2013.
4. Price, C, et al. *J Foot Ankle Res*, **7**, 40, 2014.
5. Zhang, X, et al. *J Foot Ankle Res*, **6**, 45, 2013

# THE EFFECTS OF MYOFASCIAL RELEASE AND ANKLE MOBILITY EXERCISES ON PLANTAR FASCIA THICKNESS IN DIVISION II BASKETBALL PLAYERS

Yngsdal, M., Burgess, E., Cannavan, D., Atwell-Scrivner, J., Seattle Pacific University, Seattle, WA, USA
Email: yngsdalm@spu.edu

## INTRODUCTION

The plantar fascia (PF) is sheath of connective tissue, spanning from the calcaneal tuberosity to the head of the metatarsals. It provides support along the longitudinal arch of the foot acting as a shock absorber. Excess or unnatural loading strategies can lead to plantar fasciitis.[1] Plantar fasciitis is diagnosed when the fascia thickness exceeds 4 mm[2]. Like all biological tissues, the PF will respond to loading strategies. Indeed, our laboratory has previously found increases in PF thickness throughout a basketball season in Division II college players (under review). This is likely due to high intensity training programs such as plyometric training.

At present, there is a lack of research examining preventative care modalities, especially for athletes. Thus, the purpose of this study was to compare changes in plantar fascia thickness throughout a basketball season and determine the efficacy of implementing myofascial release and ankle mobility drills.

## METHODS

Fifteen participants took part in this study, (12 females, 3 males: mean ± SD; age: 21.2 ± 1.21y.). Data were collected on three separate occasions over the course of a Division II basketball season; season start, season end, and three weeks post-season. All testing sessions occurred on a day with no practice or games. The measurements occurred in this order: 1) Plantar fascia thickness measurement using B-mode ultrasonography, 2) foot arch height measurement using the Arch Height Index measurement system, 3) hamstring flexibility, and 4) ankle joint passive range of motion measurement using a Biodex isokinetic dynamometer (Biodex, System 4 Pro). All subsequent testing sessions occurred at the same time of day (i.e. am or pm). The experimental group were randomly selected and engaged in plantar fascia myofascial release techniques and calf stretching every day before practice. The control group conducted their normal training.


**Figure 1.** Three weeks post season: plantar fascia thickness 0.37cm (3.7mm).

## RESULTS AND DISCUSSION

A repeated measures single-factor ANOVA revealed no significant changes in plantar fascia thickness within experimental group ($p>0.05$) and control group ($p> 0.05$) throughout the season. Previous research in our laboratory found significant changes in PF thickness ($p<0.01$) between session 1 and session 2, with the greatest changes found predominantly within male participants. Because of this, there may be reason to assume the plantar fascia is more likely to increase within a male population. Men are typically heavier and put more stress on their tissues during plyometric movements. The present study had a predominantly female population, which may account for the varying results. Interestingly, there was a borderline significant difference in hamstring flexibility ($p=0.06$) throughout the season. Overall, passive torque of the hamstring increased from the start of the season (37 N**.**m) to the end of the season (39.31N**.**m). If the season continued, hamstring flexibility may play a role in influencing plantar fascia thickness through the connectedness of the fascial superficial backline.

## REFERENCES

1. Roxas, M. *Alt. Medicine Review*, **10**, 83-93, 2005.
2. Chung, W, et al. *Scand. Journal of Rheum.* **29**, 255-259, 2000.

**Mean Plantar Fascia Thickness, Hamstring and Ankle Mobility Experimental Group**

| | Session 1 | Session 2 | Session 3 |
|---|---|---|---|
| PF Thickness (mm) (SD) | 4.6 (±0.082) | 4.5 (±0.096) | 4.5 (±0.087) |
| Ankle Torque (N**.**m) (SD) | 69.48 (±13.00) | 72.35 (±16.16) | 78.7 (±17.08) |
| Hamstring Torque (N**.**m) (SD) | 37.01 (±7.89) | 39.31 (±6.69) | 37.75 (±6.79) |

**Table 1.** Mean plantar fascia thickness (mm) and passive ankle and hamstring torque (N**.**m) for the experimental group (*n*=8).